

School of Natural Sciences and Mathematics

Quantum Parity Hall Effect in Bernal-Stacked Trilayer Graphene—Supplement

UT Dallas Author(s):

Fan Zhang

Rights:

©2019 The Authors. All rights reserved.

Citation:

Stepanov, P., Y. Barlas, S. Che, K. Myhro, et al. 2019. "Quantum parity Hall effect in Bernal-stacked trilayer graphene." *Proceedings of the National Academy of Sciences of the United States of America* 116(21): 10286-10290, doi: 10.1073/pnas.1820835116

This document is being made freely available by the Eugene McDermott Library of the University of Texas at Dallas with permission of the copyright owner. All rights are reserved under United States copyright law unless specified otherwise.

Supporting Information: Quantum Parity Hall Effect in ABA Graphene

Petr Stepanov,¹ Yafis Barlas,² Shi Che,¹ Kevin Myhro,³ Greyson Voigt,³ Ziqi Pi,³ Kenji Watanabe,⁴ Takashi Taniguchi,⁴ Dmitry Smirnov,⁵ Fan Zhang,⁶ R. Lake,⁷ Allan MacDonald,⁸ and Chun Ning Lau^{3,1}

¹*Department of Physics and Astronomy, Ohio State University, Columbus, OH 43220*

²*Department of Physics, Yeshiva University, New York, NY, USA*

³*Department of Physics and Astronomy, University of California, Riverside, CA 92521*

⁴*National Institute for Materials Science, 1-1 Namiki Tsukuba Ibaraki 305-0044 Japan.*

⁵*National High Magnetic Field Laboratory, Tallahassee, FL 32310.*

⁶*Department of Physics, University of Texas at Dallas, Richardson, TX 75080.*

⁷*Department of Electrical Engineering, University of California, Riverside, CA 92521*

⁸*Department of Physics, University of Texas at Austin, Austin, TX 78712-1192.*

Multi-layer graphene structures are realized by stacking 2D graphene crystals along the vertical direction. Stable structures of few-layer graphene can exist in a variety of different stacking sequences. Depending on the stacking sequence and resulting crystal symmetry, massless and massive Dirac bands can occur and even co-exist at or near neutral charge density [1].

The lattice structure is important in the determination of all multilayer graphene band structures. The lattice structure of ABA-trilayer graphene has the inequivalent atomic sites of the i^{th} graphene layer (A_i and B_i) stacked so that only half of the sub-lattice sites in each layer (B_1, A_2, B_3) have a near-neighbor in the adjacent layer, whereas the other half (A_1, B_2, A_3) don't have a near neighbor in the adjacent layers (see Fig. S1). ABA-trilayer graphene is invariant under the D_{3h} point group, which includes mirror symmetry about the middle layer. The sub-lattice orbital combinations $X_{\pm} = (X_1 \pm X_3)/\sqrt{2}$ (where $X = A, B$), form the irreducible representations of this mirror symmetry. The symmetric (anti-symmetric) combinations of the top and bottom layer orbitals X_{\pm} are even (odd) with respect to this mirror symmetry, while the middle layer X_2 orbitals have even parity. Application of an external potential difference Δ_1 between the layers breaks this mirror symmetry. As this work demonstrates, the electric field serves as an important experimental knob to analyze the symmetries of the $\nu = 0$ QH state in ABA trilayer graphene.

Non-interacting Hall conductance at $\nu = 0$

In order to understand the Landau level (LL) spectrum in ABA-trilayer graphene it is convenient to separate the Hamiltonian into contributions from subspaces with definite parity with respect to the mirror symmetry. The odd parity orbitals (A_-, B_-) exhibit a gapped Dirac-like dispersion similar to that of monolayer graphene (MLG), whereas the even parity orbitals (A_+, B_2, A_2, B_+) exhibit a band dispersion similar to gapped bilayer graphene (BLG). The gaps in the odd parity MLG and even parity BLG-like bands are due to direct interlayer remote hopping terms. The effective Hamiltonian [2] for the odd parity bands in the (A_-, B_-) basis for valley \mathbf{K} and (B_-, A_-) for valley \mathbf{K}' is given by,

$$\mathcal{H}_{\text{odd}} = \begin{pmatrix} \delta_2 - \gamma_2/2 & v\pi^\dagger \\ v\pi & -\gamma_5/2 + \delta + \delta_2 \end{pmatrix},$$

where $\pi = \pi_x + i\pi_y$ is the momentum operator in a magnetic field, $v = 3/2\gamma_0 a_0$, where $\gamma_0 = 3100$ meV and a_0 is the C-C bond distance. Here and below, γ_i parameters denote the hopping matrix elements, whose values are obtained by fitting our observations to crossing features in the LL spectrum.

In the even parity sector the direct interlayer hopping $\gamma_1 = 390$ meV pushes the even parity states (A_2, B_+) away from the neutral Fermi energy. The effective Hamiltonian [2] in terms of the low-energy bands (A_+, B_2) for valley \mathbf{K} and (B_2, A_+) for valley \mathbf{K}' is,

$$\mathcal{H}_{\text{even}} = \begin{pmatrix} \gamma_2/2 + \delta_2 & -\frac{1}{2m}(\pi^\dagger)^2 \\ -\frac{1}{2m}(\pi)^2 & -2\delta_2 \end{pmatrix} + \frac{v^2}{2\gamma_1^2} \begin{pmatrix} (\delta - 2\delta_2)\pi^\dagger\pi & 0 \\ 0 & (\gamma_5/2 + \delta + \delta_2)\pi\pi^\dagger \end{pmatrix}.$$

By fitting the LL spectrum implied by the band Hamiltonian to experiment we obtain $\gamma_2 = -14.5$ meV, $\gamma_5 = 13$ meV and $\delta = 15$ meV. The parameter δ_2 is a function of the cite energy difference between the top and bottom layers denoted Δ_1 . For balanced layers the best fit value is $\delta_2 = 5.7$ meV. Fig. S1a shows the LL band spectrum of ABA-trilayer graphene calculated with these parameter values.

For balanced layers, the total filling factor $\nu = \nu_e + \nu_o$ can be written as the sum of the local BLG-like even parity band filling factor ν_e and the MLG-like odd parity band filling factor ν_o . Important features of the LL spectrum of

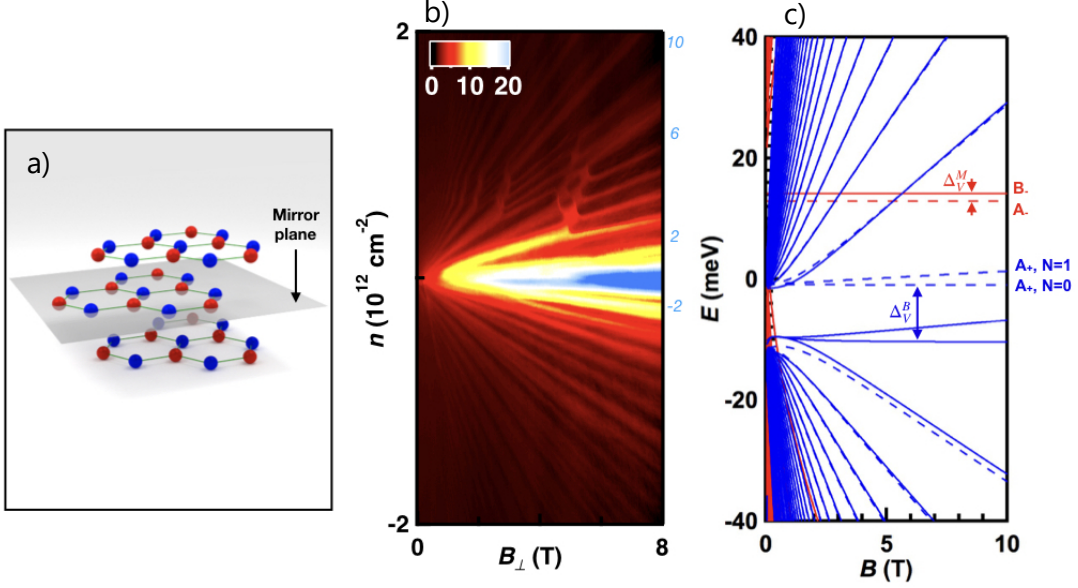


FIG. 1: (a) Crystal structure of ABA-trilayer graphene in which the middle layer is a mirror plane. (b) Landau fan diagram for ABA-trilayer graphene. Quantum mobility of the device is $\sim 80,000\text{cm}^2/(\text{Vs})$. (b). Full parameter k.p model calculations of the LL energy spectrum as a function of the B field. The dashed (solid) lines are for K (-K) valley Landau level states and the red and blue lines are for LL states arising from MLG bands that are odd under mirror reflection, and BLG-like bands that are even under mirror reflection, respectively. Note that the $N = 0$ LL energies are more weakly magnetic-field dependent and more strongly valley-dependent.

ABA trilayer graphene allow for the realization of the quantum parity Hall states at $\nu = 0$. First all LL energies except for those of the $N = 0$ states are strongly magnetic field dependent and the $N = 0$ levels have respectively four and eight flavor components for MLG and BLG. Most importantly, the odd $N=0$ level lies above the even $N = 0$ level, and the valley splitting is larger for the even $N = 0$ level than for the odd $N = 0$ level. In a single-particle theory, these properties conspire with the neutrality condition $\nu_e + \nu_o = 0$ to imply that above a very weak critical magnetic field $\nu_o = -2$ (empty odd $N = 0$ levels) and $\nu_e = +2$ (3/4 filled even $N = 0$ levels). The eigenstates and energy eigenvalues of the odd parity orbitals of the zeroth LL in the Landau gauge ($\mathbf{A} = (0, -Bx, 0)$) is given by,

$$\Phi_{0,\mathbf{K}} = \begin{pmatrix} 0 \\ \phi_{0,k_y}(\vec{x}) \end{pmatrix}; E = \delta - \gamma_5/2 + \delta_2, \quad \Phi_{0,\mathbf{K}'} = \begin{pmatrix} 0 \\ \phi_{0,k_y}(\vec{x}) \end{pmatrix}; E = -\gamma_2/2 + \delta_2,$$

where $\phi_{n,k_y}(\vec{x}) = \langle \vec{x} | n, k_y \rangle$ is the real space n^{th} LL wavefunction and each eigenstate is spin degenerate. For the zeroth LL A_- orbitals occupy the \mathbf{K}' valley and B_- orbitals the \mathbf{K} valley. The A_- orbital is at a lower energy than the B_- orbital with a valley or orbital splitting $\Delta_V^M = 1.25$ meV induced by the interlayer hopping terms, and when mirror symmetry is broken by an external displacement field also the potential energy difference between the layers.

The even parity eigenstates and corresponding energy eigenvalues for the zeroth LL are:

$$\Phi_{0,K} = \begin{pmatrix} 0 \\ \phi_{0,k_y}(\vec{x}) \end{pmatrix}; E = -2\delta_2 \quad \Phi_{1,K} = \begin{pmatrix} 0 \\ \phi_{1,k_y}(\vec{x}) \end{pmatrix}; E = -2\delta_2 + \frac{h^2 v^2}{\gamma_1^2 l_B^2} (\delta_2 + \delta + \gamma_5/2),$$

which reside completely on sublattice B_2 , and

$$\Phi_{0,K'} = \begin{pmatrix} 0 \\ \phi_{0,k_y}(\vec{x}) \end{pmatrix}; E = \gamma_2/2 \quad \Phi_{1,K'} = \begin{pmatrix} 0 \\ \phi_{1,k_y}(\vec{x}) \end{pmatrix}; E = \gamma_2/2 + \frac{h^2 v^2}{\gamma_1^2 l_B^2} (\delta - 2\delta_2),$$

which reside on sub-lattice A_+ . As before remote interlayer hopping and the energy difference between the layers determines the valley splitting in the bilayer. In the absence of a gate field $\Delta_V^B = |7.25 \text{ meV} - 3\delta_2| = 9.85 \text{ meV}$. Since $\gamma_2 > -6\delta_2$, the holes in the even parity zeroth LL reside on sub-lattice B_2 , while the electrons in the even parity zeroth LL reside on sub-lattice A_+ .

As illustrated in Fig. S1a), the conduction-band portion of the BLG-like $N = 0$ Landau level is half-occupied at neutrality, whereas the MBG-like $N = 0$ Landau level is empty. This implies that the spin degenerate gapless

edge modes of the MLG-like hole branch and the BLG-like electron branch flow in opposite directions. However the counter-propagating MLG-like hole branch and the BLG-like electron branch don't interact as long the mirror symmetry is preserved. This mirror symmetry prohibits back-scattering events, leading to a robust plateau in the two-terminal conductivity with $\sigma_{xx} = 4e^2/h$, consistent with the experimental observations. Because it breaks mirror symmetry, a displacement field that acts between the layers mixes even and odd subspaces. In the Landau gauge ($\mathbf{A} = (0, -Bx, 0)$), its projection onto the $N = 0$ subspace is

$$H_{\Delta} = \frac{\Delta_1}{2} \sum_{\sigma} (c_{A+, \sigma, X}^{\dagger} c_{A-, \sigma, X} + c_{A-, \sigma, X}^{\dagger} c_{A+, \sigma, X}), \quad (1)$$

where $\Delta_1(E)$ scales linearly with the displacement field. This terms in the Hamiltonian will introduce a gap in the edge state spectrum and allow back scattering due to disorder. This explains the rapid reduction in the longitudinal conductivity from $4e^2/h \rightarrow 0$ when a displacement field is applied.

To understand the rich phase diagram observed at higher B_{\perp} we must look more closely at the orbital character of the various LL states. The $N = 0$ odd-parity band Hamiltonian projected onto the zeroth LL is,

$$H_{odd} = \sum_{X, \tau, \sigma} \left[\frac{\Delta_{mb}}{2} + \frac{\Delta_V^M}{2} (\mathcal{I} \otimes \hat{\tau}_z) + \frac{\Delta_z}{2} (\hat{s}^z \otimes \mathcal{I}) \right] c_{\tau, \sigma, X}^{\dagger} c_{\tau', \sigma', X}, \quad (2)$$

where we have made a convenient choice for the zero of energy, the Pauli matrices $\hat{\tau}_i$ and \hat{s}_i act on the orbital/valley and spin degrees of freedom respectively, τ, σ are valley and spin labels, Δ_z is the Zeeman energy and $\Delta_{mb} = 11.5 - 3\delta_2/2 = 20.05\text{meV}$ is the even/odd parity energy splitting. Similarly for the BLG-like even parity bands we can write the zeroth LL projected band Hamiltonian as,

$$H_{even} = \sum_{X, \tau, \sigma, \alpha} \left[-\frac{\Delta_{mb}}{2} + \frac{\Delta_V^B}{2} (\mathcal{I} \otimes \hat{\tau}_z) + \frac{\Delta_z}{2} (\hat{s}^z \otimes \mathcal{I}) + \Delta_{LL}^{\tau} \delta_{\alpha, 1} \right] c_{\alpha, \tau, \sigma, X}^{\dagger} c_{\alpha', \tau, \sigma, X}, \quad (3)$$

where $\alpha, \alpha' = 0, 1$ denote the LL pseudospin orbital index in the zeroth LL, Δ_{LL}^{τ} is the orbital dependent LL pseudo-spin gap and $\delta_{\alpha, 1}$ is the Kronecker delta symbol.

Mirror symmetry in ABA-trilayer graphene

The lattice structure of ABA-trilayer graphene has a mirror symmetry with respect to the middle layer. Since ABA-trilayer is mirror symmetric the Hamiltonian $\mathcal{H} = H_{even} \otimes H_{odd}$ must commute with the mirror symmetry operator $\hat{\mathcal{M}}$. In the case of a high magnetic field, this implies that the Landau level wavefunctions can be simultaneously labeled by the eigenvalues of \mathcal{H} and $\hat{\mathcal{M}}$. Below, we describe the mirror symmetry operator for ABA trilayer graphene for spinless particles and particles with spin.

Spinless case

In general, the mirror symmetry operator $\hat{\mathcal{M}}$ can be expressed as a rotation by π with the axis of rotation perpendicular to the mirror plane, followed by an inversion. This gives $\hat{\mathcal{M}} = PD(\pi)$, where P is the inversion operator which send $\vec{r} \rightarrow -\vec{r}$, and $D(\pi)$ is the rotation operator which acts on the internal degrees of freedom such as spin. For spinless particles, this rotation matrix acts trivially and is given by the identity matrix. Under mirror symmetry the orbital in the top layer are interchanged with the orbitals in the bottom layer $\psi_{A_1} \leftrightarrow \psi_{A_3}$ and $\psi_{B_1} \leftrightarrow \psi_{B_3}$ while the orbitals in the middle layer remain unchanged $\psi_{A_2} \leftrightarrow \psi_{A_2}$ and $\psi_{B_2} \leftrightarrow \psi_{B_2}$. The mirror symmetry operator in the orbital basis can be expressed as

$$\hat{\mathcal{M}} = \begin{pmatrix} 0 & 0 & 0 & 0 & 1 & 0 \\ 0 & 0 & 0 & 0 & 0 & 1 \\ 0 & 0 & 1 & 0 & 0 & 0 \\ 0 & 0 & 0 & 1 & 0 & 0 \\ 1 & 0 & 0 & 0 & 0 & 0 \\ 0 & 1 & 0 & 0 & 0 & 0 \end{pmatrix},$$

which acts on the orbital basis $\Psi = (\psi_{A_1}, \psi_{B_1}, \psi_{A_2}, \psi_{B_2}, \psi_{A_3}, \psi_{B_3})$. In this case $\hat{\mathcal{M}}^2 = 1$ and the $\hat{\mathcal{M}}$ has the eigenvalues ± 1 .

Particles with spin

When the spin degree of freedom is included the rotation matrix operator $D(\pi)$ acts non-trivially on the spinor wavefunction. In this case the rotation operator acts on the spin degree of freedom and can be expressed as,

$$D(\pi) = \exp(-i\frac{\pi\sigma_z}{2}) = \begin{pmatrix} -i & 0 \\ 0 & i \end{pmatrix} = -i\sigma_z.$$

Combined the mirror symmetry operator for particles with spin can then be expressed as

$$\hat{\mathcal{M}} = \begin{pmatrix} -i\hat{\mathcal{M}} & 0 \\ 0 & i\hat{\mathcal{M}} \end{pmatrix},$$

which acts on the 12-component spinor $\Psi = (\Psi_\uparrow, \Psi_\downarrow)$. In the spin space $\psi_{A_1\uparrow} \leftrightarrow -i\psi_{A_3\uparrow}$ and $\psi_{A_1\downarrow} \leftrightarrow i\psi_{A_3\downarrow}$ with the same relation for the B_1 and B_3 orbital. This implies that for particles with spin $\hat{\mathcal{M}}^2 = -1$, is an anti-unitary operator. Therefore, in this case the eigenstates of different parities can be labeled by the eigenvalues $\pm i$. In particular, the eigenvalues of the $\hat{\mathcal{M}}$ for the even parity eigenstates are given by $+i(-1)^\sigma$, while the odd parity eigenstates are $-i(-1)^\sigma$, where $\sigma = \pm$ for the \uparrow (\downarrow) spins. This implies the projected mirror symmetry operator $\overline{\mathcal{M}}$ for the spin polarized state obeys $\overline{\mathcal{M}}^2 = 1$. This provides an effective Kramer degeneracy for spin states in each mirror sector.

As the magnetic field is increased electron-electron interactions within the zeroth LL significantly modify the $\nu = 0$ QH state. Interactions can lift the spin degeneracy of the $\nu = 0$ QH state while at the same time lowering the relative zero-point energy of the electron and hole LLs resulting in a QH ferromagnetic state with counter-propagating edge states with opposite spins. This results in a quantized two-terminal conductance $\sigma_{xx} = 2e^2/h$ which is protected by mirror symmetry. We discuss the effect of Coulomb interactions in the $\nu = 0$ QH state of ABA-trilayer graphene in the next section.

Interaction energy in ABA-trilayer graphene

It is well known that electron-electron interactions in graphene and semiconducting 2DEGs result in interaction induced QH plateaus not predicted by Landau quantization alone. In multi-component systems, interaction induced incompressibilities normally result from broken symmetries which lower ground state energies. In ABA-trilayer graphene these interaction induced broken symmetry ordered states compete with band gaps induced by Landau quantization. In this section, we express the mean field Hartree-Fock energy as a function of an order parameter characterizing all possible broken symmetry states in the 12-fold degenerate $N = 0$ space of ABA-trilayer graphene.

Assuming sublattice and valley independent Coulomb interactions, the interaction Hamiltonian can be expressed as,

$$\mathcal{H}_{int} = \frac{1}{2L^2} \sum_{\mathbf{q}} v_{\mathbf{q}} \rho_{\mathbf{q}} \rho_{-\mathbf{q}}, \quad (4)$$

where $v_{\mathbf{q}} = 2\pi e^2/(\epsilon q)$ and $\rho_{\mathbf{q}} = \sum_k \psi_{\mathbf{k}+\mathbf{q}, X_i, \sigma} \psi_{\mathbf{k}, X_i, \sigma}$, X_i denotes the sublattice degree of freedom for the i^{th} layer and σ is the spin and valley index. In the zeroth LL of ABA-trilayer graphene the valley and layer/sub-lattice degrees of freedom are equivalent. For balanced ABA-trilayer ($\Delta_1 = 0$) the electron density can be expressed in terms of fields with well-defined parity $\rho_{\mathbf{q}} = \rho_{\mathbf{q}}^e + \rho_{\mathbf{q}}^o$, where the $\rho_{\mathbf{q}}^i$ is the density field with even (odd) parity. In terms of even and odd parity fields the interaction Hamiltonian becomes,

$$\mathcal{H}_{int} = \frac{1}{2L^2} \sum_{\mathbf{q}} v_{\mathbf{q}} (: \rho_{\mathbf{q}}^e \rho_{-\mathbf{q}}^e : + : \rho_{\mathbf{q}}^o \rho_{-\mathbf{q}}^o :). \quad (5)$$

We neglect layer interaction anisotropy; this assumption is well justified since the ratio $d/l_B \leq 0.1$ where d is the layer spacing and l_B is the magnetic length.

To understand the role of interactions on the ordering of the broken symmetry states, we must express the Coulomb interaction in terms of the LL spectrum of ABA-trilayer graphene. For the even parity states the sublattice orbitals (B_+ and A_2) are pushed away from the Fermi energy by $\sim \gamma_1$. Therefore, at low-energies we only need the sublattice orbitals (A_+ and B_2). The Coulomb interaction projected on the zeroth LL becomes,

$$\mathcal{H}_{int} = \frac{1}{2L^2} \sum_{\mathbf{q}} v_{\mathbf{q}} (: \bar{\rho}_{\mathbf{q}}^e \bar{\rho}_{-\mathbf{q}}^e : + : \bar{\rho}_{\mathbf{q}}^o \bar{\rho}_{-\mathbf{q}}^o :), \quad (6)$$

where the projected even(odd) density operator in the Landau gauge is defined as,

$$\bar{\rho}_{\mathbf{q}}^e = \sum_{n,n',\sigma} \sum_{X,X'} F_{n,n'}(\mathbf{q}) \delta(q_y l_B^2 + X - X') e^{\frac{-iq_x}{2}(X+X')} b_{n,k_y,\sigma}^\dagger b_{n',k'_y,\sigma}, \quad (7)$$

$$\bar{\rho}_{\mathbf{q}}^o = \sum_{\sigma} \sum_{X,X'} F_{0,0}(\mathbf{q}) \delta(q_y l_B^2 + X - X') e^{\frac{-iq_x}{2}(X+X')} a_{n,k_y,\sigma}^\dagger a_{n',k'_y,\sigma}, \quad (8)$$

where $n, n' = 0, 1$ denote the extra LL index always present in BLG $N = 0$ Landau levels, σ denotes spin and valley =sublattice index, and X, X' are the guiding center quantum numbers. The b^\dagger/a^\dagger are the creation operators for the even and odd parity LLs respectively. The form factors $F_{n,n'}(\mathbf{q})$ (with $F_{00}(\mathbf{q}) = e^{-(ql_B)^2/4}$, $F_{10}(\mathbf{q}) = (iq_x + q_y)l_B e^{-(ql_B)^2/4}/\sqrt{2} = [F_{01}(-\mathbf{q})]^*$ and $F_{11}(\mathbf{q}) = (1 - (ql_B)^2/2)e^{-(ql_B)^2/4}$), reflect the character of the two different quantum cyclotron orbits in the zeroth LL. Self-energy corrections will be included to account for LL mixing justifying our projection onto the zeroth LL.

At neutrality, six of the twelve $N = 0$ Landau level orbitals are occupied. To calculate the Hartree-Fock mean field energy we therefore make the following generalized quantum Hall ferromagnetic wave function *ansatz* for the translationally invariant ground state at $\nu = 0$,

$$|\Psi_0\rangle = \prod_X \left(\prod_{i=1}^6 z_{\sigma_i}^{\alpha_i} c_{\sigma_i, X}^\dagger \right) |\Omega\rangle, \quad (9)$$

where the Einstein summation convention applies to σ_i 's and the six occupied 12-component spinors must be orthogonal. $|\Omega\rangle$ is the vacuum state in which all hole-like $N \neq 0$ Landau levels are occupied for both the even and odd parity orbitals. The partial filling of the zeroth LL is represented by an order parameter that captures the possible ordering of the broken symmetry state. The order parameter can be written as $\Delta = \sum_{\alpha} z^{\alpha} \bar{z}^{\alpha}$. To satisfy charge neutrality we impose $Tr[\Delta] = 6$ and $Tr[\Delta^2] = 6$. It is convenient to express the order parameter in terms of nine 4×4 matrices as

$$\Delta = \begin{pmatrix} \Delta_{00}^e & \Delta_{01}^e & \Delta_0^{e\sigma} \\ \Delta_{10}^e & \Delta_{11}^e & \Delta_1^{e\sigma} \\ \Delta_0^{oe} & \Delta_1^{oe} & \Delta^o \end{pmatrix}.$$

The Hartree-Fock energy of the $\nu = 0$ ground state is $E_{int} = \langle \Psi_0 | \mathcal{H}_{int} | \Psi_0 \rangle$. The mean field energy based on the wavefunction ansatz becomes,

$$\mathcal{E}_{int} = \frac{E_{int}}{N_{\phi}} = \frac{1}{2} \sum_{\{n\}_i; \sigma', \sigma} H_{n_1, n_2, n_3, n_4} Tr[\Delta_{n_1 n_4}^e] (Tr[\Delta_{n_1 n_4}^e])^2 - \frac{1}{2} X_{n_1, n_2, n_3, n_4} Tr[\Delta_{n_1 n_3}^e \Delta_{n_2 n_4}^e], \quad (10)$$

where n_i denotes the LL band index of the four-fold degenerate LLs of the odd parity bands and we define,

$$H_{n_1, n_2, n_3, n_4} = \lim_{q \rightarrow 0} v_q F_{n_1, n_4}(q) F_{n_2, n_3}(-q), \quad (11)$$

which captures the electrostatic interaction. This direct energy can be absorbed by the background and doesn't effect the broken symmetry ordering for $d/l_B \sim 0$.

$$X_{n_1, n_2, n_3, n_4} = \frac{1}{L^2} \sum_q v_q F_{n_1, n_4}(q) F_{n_2, n_3}(-q), \quad (12)$$

is the projected exchange interaction that is essential for the spontaneous ordering of the spin and valley quantum degrees of freedom. Neglecting the Hartree term, the interaction energy contribution from zeroth LL odd parity orbitals is

$$\mathcal{E}_{int}^o = \frac{E_{HF}^o}{N_{\phi}} = -\frac{1}{2} \left(X Tr[\Delta^o \Delta^o] - Tr[\Sigma^o \Delta^o] \right), \quad (13)$$

where $X = \sqrt{\pi/2}[e^2/(\epsilon l_B)]$ is the interaction exchange energy. Σ denotes the self-energy which captures the interaction of the partially filled zeroth LL with the sea of negative energy LLs. The self-energy can be defined as

$$\Sigma_{\sigma, \sigma'} = -\frac{1}{2} \sum_{n_1, n_2} X_{n_1, 0, n_2, 0} [\Delta_{n_1, n_2}^e]_{\sigma, \sigma'}, \quad (14)$$

where σ, σ' denote the four-fold spin and valley degeneracy. The interaction of the partially filled zeroth LL orbitals with the negative energy LLs results in self-energy corrections to the zeroth LLs. In single-band systems, the self-energy of the LL orbitals can be neglected by renormalization of the zero point energy. However, in multi-band systems, such as ABA trilayers, the relative self-energies can affect the ordering of the partially filled LLs. This self-energy interaction is essential for understanding the various transitions in the $\nu = 0$ state of ABA-trilayer graphene.

The mean field energy contribution from even parity orbitals can be expressed in a similar way:

$$\begin{aligned} \mathcal{E}_{int}^e = & -\frac{1}{2}X_{0000}Tr[\Delta_{00}^e\Delta_{00}^e] - \frac{1}{2}X_{1111}Tr[\Delta_{11}^e\Delta_{11}^e] - X_{0110}Tr[\Delta_{00}^e\Delta_{11}^e] \\ & - X_{0011}Tr[\Delta_{01}^e\Delta_{01}^e] + Tr[\Sigma_0^e\Delta_{00}^e] + Tr[\Sigma_1^e\Delta_{11}^e], \end{aligned} \quad (15)$$

where the zeroth LL of the even parity orbitals contains the LL pseudospin orbital degree of freedom $n = 0, 1$. We account for different self energies for the LL-pseudospin orbital Σ_α^e where $\alpha = 0, 1$ denotes the LL pseudospin orbital. The total mean field energy becomes

$$\begin{aligned} \mathcal{E}_{int} = & -\sqrt{\frac{\pi}{2}}\frac{e^2}{\epsilon l_B} \left[\frac{1}{2}Tr[\Delta_{00}^e\Delta_{00}^e] + \frac{3}{8}Tr[\Delta_{11}^e\Delta_{11}^e] + \frac{1}{2}Tr[\Delta_{00}^e\Delta_{11}^e] \right. \\ & \left. + \frac{1}{2}Tr[\Delta_{01}^e\Delta_{01}^e] + \frac{1}{2}Tr[\Delta^o\Delta^o] \right] + Tr[\Sigma^o\Delta^o] + Tr[\Sigma_0^e\Delta_{00}^e] + Tr[\Sigma_1^e\Delta_{11}^e]. \end{aligned} \quad (16)$$

The final three terms in Eq. 17 account for exchange interactions between $N = 0$ Landau level states and the negative energy sea. Because the the bare band parameters implicitly include interactions with a fully occupied set of valence band states for both MLG and BLG, this self-energy is particle-hole symmetric and positive for positive filling factors. The increase in self-energy with filling factor is the strong magnetic field counterpart of the self-energy effects that are responsible for the interaction enhancement of the velocity at the Dirac point in monolayer graphene. Its role is to lower the energy of the hole-like LLs and raise the energy of the electron-like LLs by an amount that increases monotonically with the strength of the perpendicular magnetic field B_\perp . In addition to lifting the spin, valley and LL pseudo-spin degeneracy of the zeroth LLs, interactions with therefore also tends to favor states with smaller $\nu_e = |\nu_o|$. This competition between interaction energies within the $N = 0$ manifold, the self-energy due to interactions with the negative energy sea, and the single band LL structure results in a rich phase diagram which we now relate to the experimental observations for neutral charge density $\nu = \nu_e + \nu_o = 0$ in ABA-trilayer graphene.

Phase diagram of the $\nu = 0$ QH state in ABA trilayer graphene

The experimental phase diagram of the $\nu = 0$ QH state in ABA-trilayer graphene is extremely rich. For balanced layers, the $\nu = 0$ state exhibits transition between three phases, and additional phases appear when external in-plane magnetic and displacement fields are applied. These transitions result from the magnetic field dependence of the interaction strength which yields a typical energy scale $e^2/(\epsilon l_B) \sim (56.1/\epsilon)\sqrt{B}$. For balanced layers interaction effects compete with the Landau quantization sequence determined of the band Hamiltonian. Below, we describe the symmetries of the interacting broken symmetry states and calculate their energies.

A. Quantum Parity Hall State

This first phase, which appears at low magnetic fields, exhibits a quantized value of the longitudinal conductance $\sigma_{xx} = 4e^2/h$. This phase is stabilized mainly by single-particle physics and its transport features can be understood from the LL bands of ABA-trilayer graphene. Band structure calculations show that some electron-like even parity $N = 0$ LL states are lower in energy than the hole-like odd-parity $N = 0$ LL states. Because scattering between even-parity and odd-parity states, due to either band or disorder effects, is prohibited by mirror symmetry, this state has spin degenerate counter-propagating edge modes resulting in quantization of the longitudinal conductance $\sigma_{xx} = 4e^2/h$. This state is a symmetry protected topological state and exhibits quantum parity Hall effect. When a displacement field is applied the mirror symmetry of the lattice is broken and the quantization of the diagonal conductance is destroyed. The sharp decline of the diagonal conductivity results from back-scattering events that lead to hybridization of the even and the odd parity bands. We call this state the quantum parity Hall (QPH) state.

The total filling factor is given by $\nu = \nu_e + \nu_o = 2 + (-2)$. The hole LLs have the quantum numbers (A_-, \uparrow) and (A_-, \downarrow) . However, there are two possibilities for the electron LLs $(A_+, \uparrow, 0)$ and $(A_+, \uparrow, 1)$, which is spin polarized, or $(A_+, \uparrow, 0)$ and $(A_+, \downarrow, 0)$ which is LL pseudo-spin polarized. The single particle gaps $\Delta_{LL} > \Delta_z$ and $\Delta_V^M > \Delta_z$ dictate

that the electron-like BLG LLs have the quantum numbers $(A_+, \uparrow, 0)$ and $(A_+, \downarrow, 0)$, while unoccupied the hole-like MLG LLs contain the quantum numbers (A_-, \uparrow) and (A_-, \downarrow) . The interaction energy for the QPH state is

$$\mathcal{E}_{QPH} = -\frac{15}{4} \sqrt{\frac{\pi}{2}} \frac{e^2}{(\ell_B)} - \Delta_V^B - 2\Delta_{LL} - 3\Delta_{mb} - 3\Sigma_1^e \quad (17)$$

We would like to point out that interaction effects in the even parity branch can cause a transition from the LL pseudo-spin polarized state to a spin polarized state. This state would also exhibit a quantized longitudinal conductivity $\sigma_{xx} = 4e^2/h$. However, there is no experimental evidence of this transition. As the magnetic field is increased above B_{c1} ($B_{c1} \sim 1\text{T}$) there is a transition in the longitudinal conductivity due to interaction effects, which we discuss next.

B. Quantum Parity Hall Ferromagnet

At higher fields the longitudinal conductivity is reduced to half of its non-interacting value $\sigma_{xx} = 2e^2/h$. This occurs as the combined effect of interactions within the $N = 0$ LLs and exchange interactions with the negative energy sea. As explained above, the standard regularization in which the self-energy is referenced to its value at charge neutrality points causes electron-like LLs to be raised in energy relative to hole-like LLs. If this were the only effect of interactions in the system, we expect it to drive a transition to an insulating state in which both ν_e and ν_o are zero and both diagonal and Hall conductances vanish. However the possibility of breaking spin degeneracy leads first to a state in which ν_e and $|\nu_o|$ are first reduced from two to one, and the bulk state is spontaneously spin-polarized. Because ν_e is positive its edge state has majority spin character, whereas ν_o has a counter-propagating minority spin edge channel because its filling factor is negative. This state is actually a spin Hall state since it has bulk Hall conductivities with opposite sign for opposite spins. Its longitudinal conductance is reduced from $\sigma_{xx} = 4e^2/h$ in the quantum parity Hall state to $\sigma_{xx} = 2e^2/h$. The robust quantization in the longitudinal conductivity is still protected by the mirror symmetry of the crystal lattice. As before a displacement field destroys this state because it enables hybridization and localization of counter-propagating edge states. We call this state the quantum parity Hall ferromagnet (QPHF).

The QPHF state has $\nu = 1 + (-1)$, one occupied electron-like BLG LL, and one occupied hole-like MLG LL. Counter-propagating even parity spin-up electrons and odd parity spin-down holes at the edge lead to vanishing Hall conductance and a diagonal conductivity that is twice the conductance quantum. The occupied electron-like BLG LL has the quantum numbers (A_+, \uparrow) , while the occupied hole-like MLG LL the quantum numbers (A_-, \downarrow) . The ground state energy is,

$$\mathcal{E}_{QPHF} = -\frac{15}{4} \sqrt{\frac{\pi}{2}} \frac{e^2}{(\ell_B)} - \frac{3}{2} \Delta_V^B - 2\Delta_{LL} - 2\Delta_{mb} - \frac{\Delta_V^M}{2} - \Delta_Z - \Sigma_0^e - 2\Sigma_1^e - \Sigma^o. \quad (18)$$

As mentioned above, this quantum spin Hall-like state has counter-propagating even and odd parity edge state branches with opposite spin quantum numbers. However, unlike the quantum spin Hall state, in this state the quantization of the longitudinal conductivity is due to the mirror symmetry and not time reversal symmetry which applies to the former. As the mirror symmetry is broken the counter-propagating spin intermix resulting in the destruction of the plateau in the longitudinal conductivity. The spins intermix due to the presence of a Rashba spin orbit interaction, which is allowed as the displacement field is increased. Because the edge states are gapless a very small Rashba spin-orbit coupling leads to backscattering of the counterpropagating spin and hence localization of the edge states.

By comparing to experiment, the mean field energy expression can be used to determine the strength of exchange interactions with the negative energy sea. In order for the QPHF state to be lowest energy in energy the condition $\mathcal{E}_{QPHF} \leq \mathcal{E}_{QPH}$ must be satisfied. This implies that

$$\Sigma_0^e + \Sigma^o \geq \Delta_{mb} - \frac{\Delta_V^M + \Delta_V^B}{2} - \Delta_z = 14.5\text{meV} - \Delta_z. \quad (19)$$

This inequality is satisfied for the $B \geq B_{c1}$ (where B_{c1} is the critical magnetic field for the QPH \rightarrow QPHF transition). The right-hand side only involves the remote hopping band parameters and the Zeeman energy. Since the exchange energy is same for both broken symmetry states it cancels out. The above condition shows that this transition can be tuned by the magnetic field. Since the self-energy monotonically increases with B_{\perp} , we expect this to occur as the magnetic field is increased.

C. Quantum Valley Ferromagnetic Insulator

As the perpendicular magnetic field is increased the longitudinal conductance eventually transitions from $2e^2/h \rightarrow 0$. For $B_\perp > 6\text{T}$, ABA-trilayer graphene is a quantum valley ferromagnetic insulator (QVFI). In this state, the odd parity hole-like LLs move below the Fermi energy and the even parity electron-like LLs move above the charge neutrality point. When this happens there is a clear gap at the Fermi energy which simply gives an insulator. Since there are no edge states at the Fermi level, $\sigma_{xx} \rightarrow 0$. The even and odd parity occupied LLs are both valley polarized and there is therefore a bulk valley Hall effect.

In this state, all the hole-like LLs for both even and odd parity are occupied whereas the electron-like LLs are unoccupied. The occupied even parity LLs have the quantum numbers (B_2, n, σ) , for both $n = 0, 1$ and $\sigma = \uparrow, \downarrow$, while the odd parity LL have the quantum numbers (A_-, σ) . The ground state energy of the QVFI is

$$\mathcal{E}_{QVFI} = -\frac{15}{4} \sqrt{\frac{\pi}{2}} \frac{e^2}{(\epsilon l_B)} - 2\Delta_V^B - 2\Delta_{LL} - \Delta_{mb} - \Delta_V^M - 2\Sigma_0^e - 2\Sigma_1^e - 2\Sigma^o \quad (20)$$

Again comparison of the ground state energies $\mathcal{E}_{QPHF} \geq \mathcal{E}_{QVFI}$ gives a condition on the self-energies

$$\Sigma_0^e + \Sigma^o \geq \Delta_{mb} + \Delta_Z - \frac{\Delta_V^M + \Delta_V^B}{2} = 14.5\text{meV} + \Delta_z, \quad (21)$$

with the equality satisfied for $B = B_{c2}$ (B_{c2} is the critical field for the transition from the QPHF state to the QVFI). Again, the self-energy conditions for both transitions depend on the Zeeman energy and the band parameters which are independent of the magnetic field. Therefore, the Zeeman energy causes the transition from the QPHF state to the QVFI. Since the Zeeman energy is small the combined inequalities also indicate that the sum of the self energies is weakly dependent on B_\perp . The condition derived above also suggests that this transition can be reversed by fixing B_\perp in the insulating region and varying the total magnetic field. This was done by adding an in-plane magnetic field, we discuss this in the next.

D. Effect of in plane field in the QVF insulator

The spin-polarized QPHF state is stabilized relative to the QVFI state by the Zeeman energy which is proportional to the total magnetic field $B = \sqrt{B_\perp^2 + B_\parallel^2}$. Since the interaction self-energies are dependent on B_\perp and other band parameters are magnetic-field independent, the region of stability of the QPHF state can be enhanced by increasing the in-plane magnetic field. As before, for balanced layers ($\Delta_1 = 0$), mirror symmetry still protects the counter-propagating states. However, the spins of the counter-propagating edge states is now canted towards the direction of the total magnetic field.

Phase diagram as a function of the displacement field

At high electric field the $\nu = 0$ QH state exhibits insulating character $\sigma_{xx} \rightarrow 0$. The QH state at high electric field must be layer polarized. For balanced layer or zero electric field the odd parity LL MLG-like bands are anti-symmetric combinations of the top and the bottom layers for both the A and the B sub-lattices, while the even parity BLG-like bands consist of electrons on the B sub-lattice in the middle layer and the symmetric combination of the A sublattices in the top and the bottom layers. At high electric fields, the electrons prefer to occupy the top most layers. In the zeroth LL, the electric field acts like a tunneling term between even and odd parity states. At low fields, this transition to a layer polarized state from both QPH phase and the QPHF phase is already pre-empted by the edge state localization effects. However, in the case of QVF state which is already an insulator, the transition to the another bulk insulating state appears as a peak in the diagonal conductivity and the bulk state is changed.

For $B_\perp > B_{c2}$ the $\nu = 0$ QH state goes through an insulator-insulator transition as a function of the electric field. This bulk transition is due to partial layer polarization and we refer to this state as the partially layer polarized (PLP) state. In the QVF insulating state the reorganization of the even parity electron and odd parity hole LLs occurs due to the interactions. Hence, the incompressible energy gaps due to the interactions scale as square root of the magnetic field. For the layer polarized state energy contribution from the electric field must overcome this interaction energy for a transition to a layer polarized bulk state. Based on the above arguments it is easy anticipate that this phase boundary in the E vs B_\perp must scale as $\sqrt{B_\perp}$ consistent with the experimental observation. This dependence of the phase boundary can be precisely calculated from our expression of the ground state energy. In the PLP state

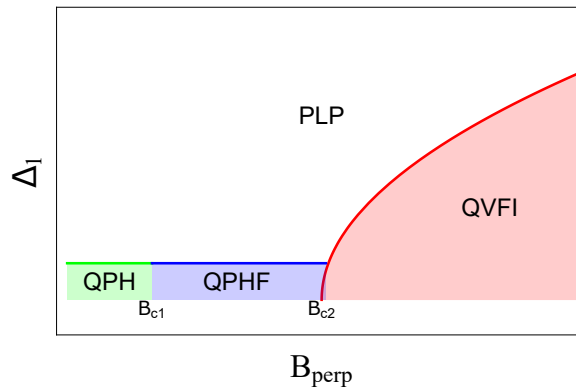


FIG. 2: Schematic phase diagram of the $\nu = 0$ QH state in ABA-trilayer graphene. Phase I is the quantum parity Hall (QPH) state, Phase II is the quantum parity Hall ferromagnetic (QPHF) state, Phase III is the quantum valley ferromagnetic insulator (QVFI) and Phase IV is the partially layer polarized state (PLP) state. The critical fields for the QPH \rightarrow QPHF \rightarrow QVFI are denoted by B_{c1} and B_{c2} respectively.

the electron occupation below the Fermi energy is given by the quantum numbers $(0, A_1, \uparrow; 0, A_1, \downarrow; 0, B_2, \uparrow; 0, B_2, \downarrow; 1, B_2, \uparrow; 1, B_2, \downarrow)$. The ground state energy is given by

$$\mathcal{E}_{PLP} = -\frac{11}{4} \sqrt{\frac{\pi}{2}} \frac{e^2}{(\epsilon l_B)} - \frac{\Delta_V^B}{2} - 2\Delta_{LL} - 2\Delta_{mb} - \frac{\Delta_V^M}{2} - \Delta_1 + \Sigma_0^e - 2\Sigma_1^e - \Sigma^o \quad (22)$$

Again comparison of the ground state energies $\mathcal{E}_{QVFI} \geq \mathcal{E}_{PLP}$ gives a condition on the self-energies

$$3\Sigma_0^e + \Sigma^o \leq -\sqrt{\frac{\pi}{2}} \frac{e^2}{(\epsilon l_B)} + \Delta_{mb} + \Delta_1 - \frac{\Delta_V^M + 3\Delta_V^B}{2}, \quad (23)$$

which has a strong dependence of the on the exchange interaction. Since we already know that the self-energy has a weak dependence on B_{\perp} we can estimate the phase boundary from the above condition

$$\Delta_1 \simeq \sqrt{\frac{\pi}{2}} \frac{e^2}{(\epsilon l_B)} + \Delta_V^B + 2\Sigma_0^e. \quad (24)$$

As anticipated the exchange interaction scaling $\sim \sqrt{B_{\perp}}$ determines the phase boundary of the two competing states. Combining all this one arrives at the schematic phase diagram shown in Fig. 2

-
- [1] Barlas Y., Yang K. and MacDonald A. H. Quantum Hall effects in graphene-based two-dimensional electron systems, *Nanotechnology* **23**, 052001 (2012).
 [2] Serbyn M. and Abanin D. A. New Dirac points and multiple Landau level crossings in biased trilayer graphene, *Phys. Rev. B* **87**, 115422 (2013).